

Calculations were also carried out with  $Z = 6$  and the values of  $\Delta A$  obtained are about 3.5% smaller.

Within the experimental errors the values of  $\Delta A_1$  in mixtures of two nitrates (a and b) obey the linear relation<sup>7</sup>

$$\Delta A_1(\text{mixture}) = x_a \Delta A_1(\text{in pure a}) + x_b \Delta A_1(\text{in pure b}) \quad (6)$$

where  $x$  is the mole fraction of the nitrates. This equation was found to be followed by the  $\text{Cl}^-$  and  $\text{Br}^-$  complexes of  $\text{Ag}(\text{I})$  in  $\text{NaNO}_3$  and  $\text{KNO}_3$  mixtures. In spite of the large difference between the ionic radii of  $\text{Li}^+$  and  $\text{K}^+$  this relation was used to calculate the value of  $\Delta A_1$  for the  $\text{Cl}^-$  and  $\text{Br}^-$  complexes of  $\text{Ag}(\text{I})$  in pure  $\text{LiNO}_3$  melt using the values of  $\Delta A_1$  for pure  $\text{KNO}_3$  obtained by Manning, *et al.*,<sup>8</sup> and assuming that they are independent of temperature. The values found are given in Table IV together with the values for other melts. The values of  $-\Delta A_1$  for the pure  $\text{LiNO}_3$  melt seem large

(7) M. Blander in "Molten Salt Chemistry," M. Blander, Ed., Interscience Publishers, New York, N. Y., 1964, p 127 ff.

(8) D. L. Manning, J. Braunstein, and M. Blander, *J. Phys. Chem.*, **66**, 2069 (1962).

when compared with those for pure  $\text{NaNO}_3$  or  $\text{KNO}_3$ . This type of anomalous behavior of the melts containing  $\text{LiNO}_3$  has also been observed in the formation of  $\text{CdBr}^+$  and  $\text{CdBr}_2^0$  and  $\text{AgCl}^{10}$  complexes in  $\text{LiNO}_3$ - $\text{KNO}_3$  mixtures. In these systems the values of  $-\Delta A_i$  become larger as the mole fraction of  $\text{LiNO}_3$  increases and the values are larger than in the corresponding  $\text{NaNO}_3$ - $\text{KNO}_3$  mixtures. These anomalous effects have been explained on the basis of a smaller effective radius of the nitrate ion in lithium-containing melts.<sup>9-11</sup> Thomas and Braunstein<sup>10</sup> have pointed out some of the difficulties of emf measurements at high lithium nitrate concentration and the solubility method reported here may be more effective for exploring high lithium systems.

**Acknowledgment.**—Much of the experimental work was carried out with the aid of Mrs. M. Sie. This work has been supported by the U. S. Atomic Energy Commission, Contract No. AT-(30-1)-305.

(9) J. Braunstein and A. S. Minano, *Inorg. Chem.*, **3**, 218 (1964).

(10) C. Thomas and J. Braunstein, *J. Phys. Chem.*, **68**, 957 (1964).

(11) S. V. Meschel and O. J. Kleppa, *ibid.*, **68**, 3840 (1964).

CONTRIBUTION FROM THE DEPARTMENTS OF CHEMISTRY, FACULTY OF SCIENCE, THE UNIVERSITY OF TOKYO, HONGO, TOKYO, JAPAN, AND FACULTY OF SCIENCE, THE UNIVERSITY OF NAGOYA, CHIKUSA, NAGOYA, JAPAN

## Low-Temperature Far-Infrared Spectra of Hexanitro Complex Salts<sup>1</sup>

BY ICHIRO NAKAGAWA,<sup>2a</sup> TAKEHIKO SHIMANOUCI,<sup>2a</sup> AND KAZUO YAMASAKI<sup>2b</sup>

Received January 19, 1968

Far-infrared spectra of  $\text{M}_3[\text{Co}(\text{NO}_2)_6]$  ( $\text{M} = \text{Na}, \text{K}, \text{Rb}, \text{and Cs}$ ) and  $\text{M}'_2\text{M}''[\text{Ni}(\text{NO}_2)_6]$  ( $\text{M}' = \text{K and Na}; \text{M}'' = \text{Ca and Ba}$ ) have been measured down to  $50 \text{ cm}^{-1}$  at room temperature and liquid nitrogen temperature. Lattice vibrations due to the displacements of the outer cations relative to the complex ion are observed below  $200 \text{ cm}^{-1}$ . Those frequencies change depending upon the mass of the cations and the interionic potential constants. The far-infrared bands due to the lattice vibrations and the intramolecular vibrations in the complex ion were both interpreted for  $\text{M}_3[\text{Co}(\text{NO}_2)_6]$  and  $\text{K}_2\text{Ca}$ - and  $\text{K}_2\text{Ba}[\text{Ni}(\text{NO}_2)_6]$  by the normal-coordinate analysis of the crystal as a whole, on the basis of the  $\text{T}_h$ <sup>3</sup> structure determined by the X-ray analysis, only the interaction between the outer cations and the oxygen atoms being taken into account.  $\text{Na}_3[\text{Co}(\text{NO}_2)_6]$  reveals quite a different spectrum from those for the other complex salts, in the lattice vibration region as well as in the intramolecular vibration region. This complex spectrum has been interpreted satisfactorily on the basis of the  $\text{C}_{3i}$  deformed structure.

### Introduction

In a previous report we discussed the lattice vibrations of hexanitrocobalt(III) complex salts.<sup>3</sup> We also reported that the Na salt revealed a much more complicated spectrum than the K, Rb, and Cs salts.<sup>3,4</sup> From the viewpoint of the intramolecular vibrations we concluded that the  $\text{Co}(\text{NO}_2)_6^{3-}$  ion in the Na salt has  $\text{C}_{3i}$  ( $\text{S}_6$ ) symmetry instead of  $\text{T}_h$  symmetry.<sup>4a</sup>

A far-infrared spectral measurement at liquid nitrogen temperature has recently enabled us to obtain more distinct bands than those at room temperature and we

have obtained well-defined far-infrared spectra in the region down to  $50 \text{ cm}^{-1}$  at low temperature as well as room temperature for a series of  $\text{M}_3[\text{Co}(\text{NO}_2)_6]$  compounds ( $\text{M} = \text{Na}, \text{K}, \text{Rb}, \text{and Cs}$ ). A similar measurement has been extended to the hexanitronickel(II) complex salts such as  $\text{K}_2\text{Ca}[\text{Ni}(\text{NO}_2)_6]$ ,  $\text{K}_2\text{Ba}[\text{Ni}(\text{NO}_2)_6]$ , and  $\text{Na}_2\text{Ba}[\text{Ni}(\text{NO}_2)_6]$ .

In the present paper we give the summary of the experimental results and discuss the nature of the lattice vibrations as well as the intramolecular vibrations, on considering the frequency shifts with the lowering of temperature. A normal-coordinate analysis of  $\text{Na}_3[\text{Co}(\text{NO}_2)_6]$  has been made on the basis of the structure with the space group  $\text{C}_{3i}$ , without separating the lattice vibrations and the intramolecular vibrations in the  $\text{Co}(\text{NO}_2)_6^{3-}$  ion. These results yield important infor-

(1) Presented before the 10th International Conference on Coordination Chemistry, Nikko, Japan, Sept 1967.

(2) (a) The University of Tokyo; (b) The University of Nagoya.

(3) I. Nakagawa and T. Shimanouchi, *Spectrochim. Acta*, **22**, 1707 (1966).

(4) (a) I. Nakagawa, T. Shimanouchi, and K. Yamasaki, *Inorg. Chem.*, **3**, 772 (1964); (b) I. Nakagawa and T. Shimanouchi, *Spectrochim. Acta*, **23A**, 2099 (1967).

mation regarding the interaction between the complex ion and the outer cations.

### Experimental Section

**Samples.**— $\text{Rb}_3[\text{Co}(\text{NO}_2)_6]$  and  $\text{Cs}_3[\text{Co}(\text{NO}_2)_6]$  were prepared by the reaction of  $\text{RbCl}$  and  $\text{CsCl}$  with  $\text{Na}_3[\text{Co}(\text{NO}_2)_6]$ , respectively. The colors of these samples are lemon yellow.

$\text{K}_2\text{Ba}[\text{Ni}(\text{NO}_2)_6]$  and  $\text{K}_2\text{Ca}[\text{Ni}(\text{NO}_2)_6]$  were prepared by the method given in the literature.<sup>5,6</sup> The former is lemon yellow and the latter is brownish yellow.

**Measurement of Spectra.**—A Hitachi FIS-1 vacuum far-infrared spectrophotometer ( $500\text{--}50\text{ cm}^{-1}$ ) was used. The samples dispersed in a polyethylene sheet and a Nujol mull were used for the measurement of far-infrared spectra. Low-temperature measurements at liquid nitrogen temperature were made for the Nujol mull samples inserted into the two silicon plates contacted with the metal conductor in the low-temperature cell.<sup>7</sup> Observed low-temperature spectra are reproduced in Figures 1 and 2.

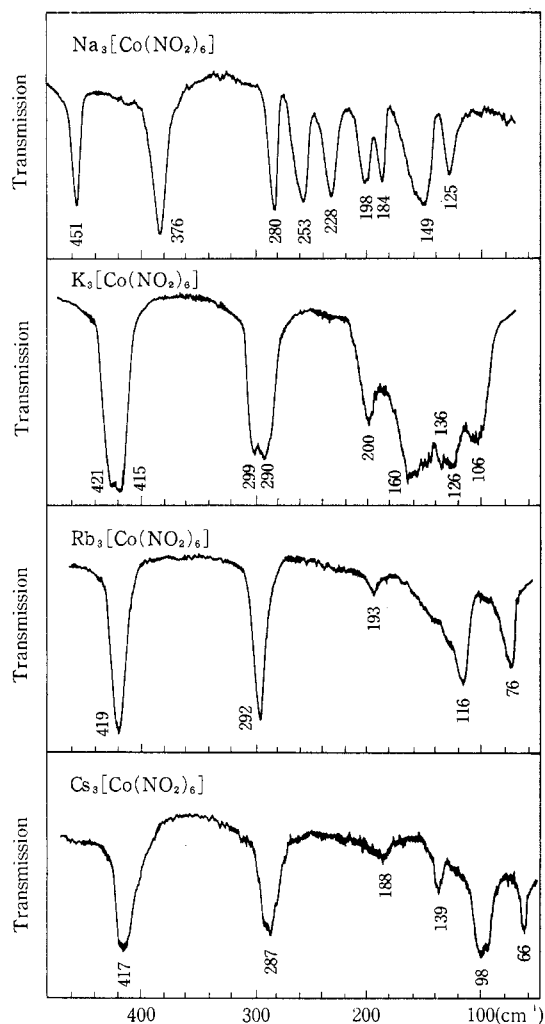


Figure 1.—Far-infrared spectra of hexanitrocobalt(III) complex salts (Nujol mull) at liquid nitrogen temperature.

**Observed Frequencies.**—Spectral measurements are limited to the transmittance, and throughout this study we regard the absorption frequencies obtained from the transmittance of the powder samples as  $\nu_0$ 's (resonance frequencies or the minimum transmission frequencies as a thickness  $d \rightarrow 0$ ). The difference

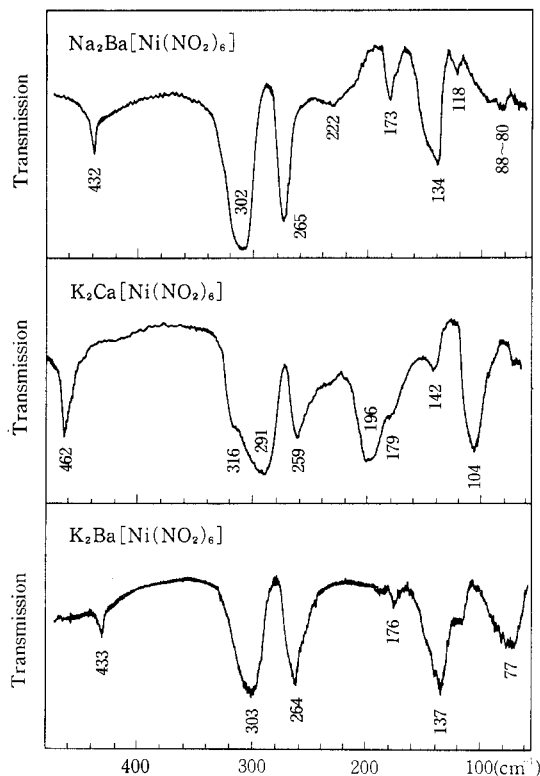


Figure 2.—Far-infrared spectra of hexanitronickel(II) complex salts (Nujol mull) at liquid nitrogen temperature.

between the resonance frequencies obtained from the reflection data of a crystal and those from the transmission data of a powder sample is less than 5% for the lattice vibrations of an ionic crystal such as  $\text{KNiF}_3$  and  $\text{KMgF}_3$ , according to the results by Perry, *et al.*<sup>8</sup>

For ionic cubic crystal systems the transverse and longitudinal optical modes may be split. However, the transverse frequencies  $\nu_t$ 's correspond to the resonance frequencies  $\nu_0$ 's and accordingly the observed values here may be regarded as  $\nu_t$ 's which can be determined by the local restoring forces on the basis of the model of the molecular dynamics.

### Results and Discussion

(1)  $\text{M}_3[\text{Co}(\text{NO}_2)_6]$  ( $\text{M} = \text{K}, \text{Rb}, \text{and Cs}$ ).—The crystal structure is cubic with the space group  $\text{T}_h^3$  as shown in Figure 3.<sup>9,10</sup> The Bravais unit cell is composed of 22 atoms,  $\text{M}_3[\text{Co}(\text{NO}_2)_6]$ , one complex ion ( $\text{Co}(\text{NO}_2)_6^{3-}$ ), and three outer cations ( $3\text{ M}^+$ ). The result of the factor group analysis is shown in Table I, from which ten vibrations of the  $\text{F}_u$  species are expected to be observed in the infrared spectra. The spectra shown in Figure 1 in the region below  $500\text{ cm}^{-1}$  reveal six bands for these complex salts. In the higher frequency region not shown here there are four bands, corresponding to the  $\text{NO}_2$  symmetric and antisymmetric stretching,  $\text{NO}_2$  scissoring, and  $\text{NO}_2$  wagging modes; therefore, the total number of the observed infrared bands is 10 as expected in Table I. The bands for each complex become sharp and shift to the higher frequency side with lowering temperature. In the region below  $150\text{ cm}^{-1}$  there are

(8) G. R. Hunt, C. H. Perry, and J. Ferguson, *Phys. Rev.*, **134**, A688 (1964); C. H. Perry, *Japan. J. Appl. Phys., Suppl. 1*, **4**, 564 (1965).

(9) M. Driel and H. J. Verwell, *Z. Krist.*, **A95**, 308 (1936).

(10) R. W. G. Wyckoff, "The Structure of Crystals," Vol. II, Interscience Publishers, Inc., New York, N. Y., 1951, Chapters IX and X

(5) D. M. L. Goodgame, *Inorg. Chem.*, **3**, 1389 (1964).

(6) A. Rosenheim and I. Koppel, *Z. Anorg. Allgem. Chem.*, **17**, 35 (1898).

(7) I. Harada and T. Shimanouchi, *J. Chem. Phys.*, **46**, 2708 (1967).

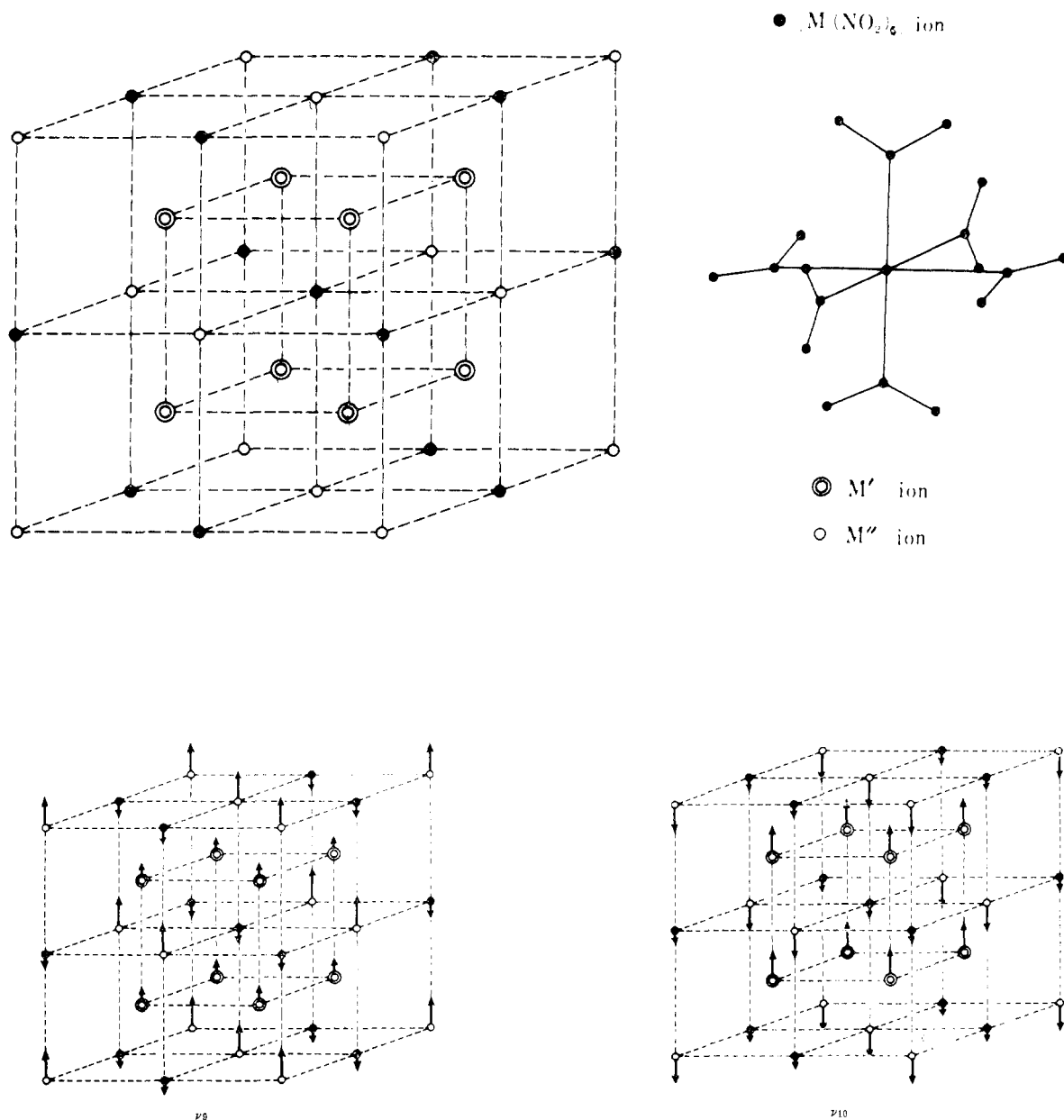


Figure 3.—Structure of hexanitro complex salts with the space group  $T_h^3$  and approximate modes of lattice vibrations  $\nu_9$  and  $\nu_{10}$ .

TABLE I  
FACTOR GROUP ANALYSIS OF  
 $M_3[Co(NO_2)_6]$  (K, Rb, and Cs)<sup>a</sup>

| $T_h^3$ | $N$ | $T$ | $T'$ | $R'$ | $n$ |    |
|---------|-----|-----|------|------|-----|----|
| $A_g$   | 3   | 0   | 0    | 0    | 3   | R  |
| $A_u$   | 1   | 0   | 0    | 0    | 1   | ia |
| $E_g$   | 3   | 0   | 0    | 0    | 3   | R  |
| $E_u$   | 1   | 0   | 0    | 0    | 1   | ia |
| $F_g$   | 7   | 0   | 1    | 1    | 5   | R  |
| $F_u$   | 11  | 1   | 2    | 0    | 8   | ir |

<sup>a</sup> Symbols:  $N$ , number of the total freedoms;  $T$ , number of the acoustical translational motions;  $T'$ , number of the optical translational lattice vibrations;  $R'$ , number of the rotational lattice vibrations;  $n$ , number of the intramolecular vibrations of  $Co(NO_2)_6^{3-}$  ion; R, Raman active; ir, infrared active; ia, inactive.

two bands which change their frequencies considerably with the outer cations (132, 109, 94  $cm^{-1}$  and 106, 74, 63  $cm^{-1}$ , for K, Rb, and Cs salts, respectively). They

may primarily arise from the lattice vibrations due to the interaction between the complex ion and the outer cations.

The optically active vibration frequencies of the crystal are calculated according to the procedure described in previous papers,<sup>3,11</sup> by using the potential function  $V = V_{intra} + V_{inter}$ , where  $V_{intra}$  denotes the intramolecular potential in the complex ion, which we have discussed in several of our previous papers.<sup>4b,12-14</sup> The values of the intramolecular force constants used in the calculation are listed in the Appendix.  $V_{inter}$  denotes the interionic interaction potential and we assume that this term arises from the interaction between the  $M^+$  ions and the neighboring O atoms. For

(11) T. Shimanouchi, M. Tsuboi, and T. Miyazawa, *J. Chem. Phys.*, **35**, 1597 (1961).

(12) I. Nakagawa and T. Shimanouchi, *Spectrochim. Acta*, **22**, 759 (1966).

(13) T. Shimanouchi and I. Nakagawa, *Inorg. Chem.*, **3**, 1805 (1964).

(14) J. Hiraiishi, I. Nakagawa, and T. Shimanouchi, *Spectrochim. Acta*, **20**, 819 (1964).

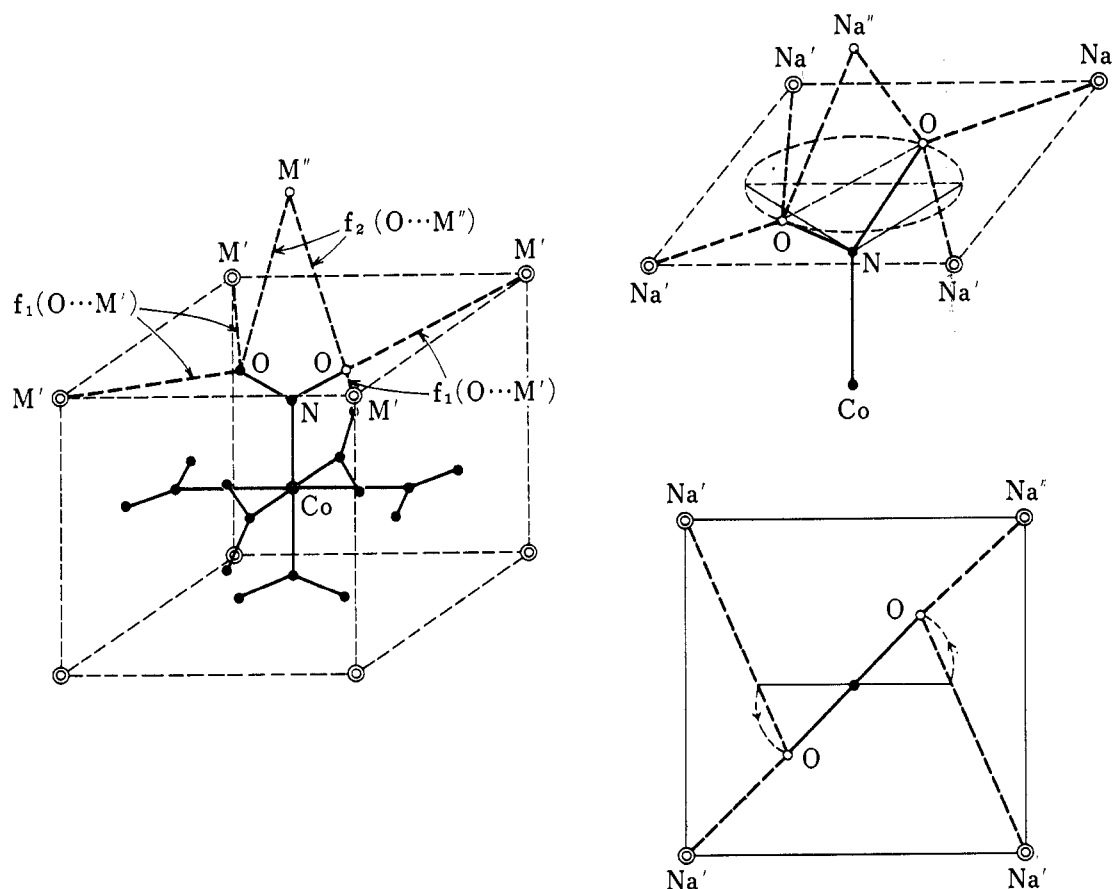


Figure 4.—Positions of oxygen atoms and outer cations for  $M_3[Co(NO_2)_6]$  ( $M = K, Rb, \text{ and } Cs$ ) and  $Na_3[Co(NO_2)_6]$ .

these complex salts the nearest and the second nearest  $M^+ \cdots O$  distances are 2.80–3.15 Å ( $q_2(M'' \cdots O)$ ) and 3.05–3.30 Å ( $q_1(M' \cdots O)$ ), respectively (see Figure 4 and Table II). The interaction between the atoms whose distances are longer than 3.5 Å is not taken into consideration.

The calculated frequencies and the interionic potential constants are shown in Table II, where only the vibration frequencies of the  $F_u$  species are given to save space. We can see that the observed bands for this series of complex salts are explained satisfactorily by the above potential function and by the use of the interionic potential constants  $f(M^+ \cdots O)$  of ca. 0.1 mdyn/Å which change slightly depending upon the interatomic distances.

The displacement of each atom is obtained from the elements of the  $L_x$  matrix (the eigenvector of the  $M^{-1}F_x$  matrix and the transformation matrix between the Cartesian displacement coordinates  $X$  and the normal coordinates  $Q$ ,  $X = L_x Q$ ).<sup>2</sup> We can see from this calculation that  $M'$  and  $M''$  displace in the same direction for the  $\nu_9$  mode and in the opposite direction for the  $\nu_{10}$  mode, though in the  $\nu_9$  vibration for the K and Rb salts the lattice modes are coupled appreciably with the intramolecular modes. A sketch of the approximate motion is given in Figure 3.

(2)  $Na_3[Co(NO_2)_6]$ .—No structural analysis has been made for this complex salt. As shown in Figures 1 and 2 the spectrum of the Na salt is quite different

TABLE II  
Observed and Calculated Frequencies  
( $cm^{-1}$ ) of  $M_3[Co(NO_2)_6]$  Salts

| $T_h^h$<br>$F_u$ | $K_3[Co(NO_2)_6]$ |       | $Rb_3[Co(NO_2)_6]$ |       | $Cs_3[Co(NO_2)_6]$ |       | Vib modes                                |
|------------------|-------------------|-------|--------------------|-------|--------------------|-------|--|
|                  | Obsd              | Calcd | Obsd               | Calcd | Obsd               | Calcd |  |
| $\nu_1$          | 1386              | 1393  | 1399               | 1393  | 1400               | 1393  | $NO_2$ antisym str                       |
| $\nu_2$          | 1332              | 1325  | 1327               | 1325  | 1326               | 1325  | $NO_2$ sym str                           |
| $\nu_3$          | 827               | 818   | 827                | 818   | 832                | 817   | $NO_2$ scissor                           |
| $\nu_4$          | 637               | 619   | 633                | 619   | 630                | 618   | $NO_2$ wag                               |
| $\nu_5$          | 416               | 421   | 413                | 421   | 409                | 420   | Co–N str                                 |
| $\nu_6$          | 293               | 293   | 287                | 288   | 281                | 286   | $NO_2$ rock and skel def                 |
| $\nu_7$          | 195               | 201   | 191                | 181   | 186                | 170   | Skel def and $M'$ lattice                |
| $\nu_8$          | 154               | 157   | 141                | 149   | 136                | 141   | Skel def, $NO_2$ rock, and $M''$ lattice |
| $\nu_9$          | 132               | 162   | 109                | 117   | 94                 | 95    | $M''$ and $M'$ lattice                   |
| $\nu_{10}$       | 106               | 106   | 74                 | 76    | 63                 | 59    | $M'$ and $M''$ lattice                   |

Interionic Potential Constants and Interatomic Distances of  $M_3[Co(NO_2)_6]$  Salts

|                | $K^+ \cdots O$ | $Rb^+ \cdots O$ | $Cs^+ \cdots O$ |
|----------------|----------------|-----------------|-----------------|
| $f_1$ , mdyn/Å | 0.11           | 0.10            | 0.08            |
| $q_1$ , Å      | 3.05           | 3.15            | 3.30            |
| $f_2$ , mdyn/Å | 0.14           | 0.12            | 0.10            |
| $q_2$ , Å      | 2.83           | 2.95            | 3.15            |

from those for the K, Rb, and Cs salts. In the previous note we attributed this remarkable difference in the spectrum to the lowering of the symmetry of the  $Co(NO_2)_6^{3-}$  ion from  $T_h$  to  $C_{3i}$  ( $S_6$ ) through the analysis of

the intramolecular vibrations (see Figure 1 of ref 4a). This  $C_{3i}$  structure where the  $NO_2$  plane rotates about the Co-N axis may be understood by the smaller ionic radius of the  $Na^+$  ion, since for the  $T_h$  structure four interatomic distances,  $q_1(Na' \cdots O)$  in Figure 4, are too large to form a stable crystal. When the  $Co(NO_2)_6^{3-}$  ion takes a  $C_{3i}$  structure, two of the  $q_1(Na' \cdots O)$  distances become shorter and a stable crystal may be formed (see Figure 4). In order to see whether this  $C_{3i}$  structure may explain the lattice frequencies as well as the intramolecular vibration frequencies for the Na salt, we made a calculation of optically active vibrational frequencies of crystal as a whole. In our assumed structure,  $Na^+$  cations and Co atoms are located at the lattice points as shown in Figure 3 as in the case of a cubic crystal. However, owing to the twisting of the  $NO_2$  plane, the crystal structure is no longer cubic. On the basis of the  $C_{3i}$  structure with a twisting angle of  $30^\circ$  and  $a = 10.00 \text{ \AA}$ , the interatomic distances  $q(Na \cdots O)$  are calculated as:  $q_1(Na' \cdots O) = 2.55 \text{ \AA}$ ,  $q_1'(Na' \cdots O) = 3.42 \text{ \AA}$ , and  $q_2(Na'' \cdots O) = 2.62 \text{ \AA}$  (see Figure 4).

The result of the factor group analysis is shown in Table III, from which both  $A_u$  and  $E_u$  vibrations are expected to appear in the infrared spectrum. In the  $A_u$  and  $E_u$  species two  $NO_2$  twisting modes are included, whose intensities may be very weak. The calculated frequencies are given in Table IV, together with the interionic potential constants, where those for the  $A_g$  and  $E_g$  species are not included to save space. In this calculation the intramolecular force constants are the same as those for the K, Rb, and Cs salts (see Appendix). We can see in Table IV that the calculated frequencies for the  $C_{3i}$  crystal structure correspond with the observed frequencies.

TABLE III  
FACTOR GROUP ANALYSIS OF  $Na_3[Co(NO_2)_6]^a$

| $C_{3i}$ | $N$ | $T$ | $T'$ | $R'$ | $n$ |    |
|----------|-----|-----|------|------|-----|----|
| $A_g$    | 10  | 0   | 1    | 1    | 8   | R  |
| $A_u$    | 12  | 1   | 2    | 0    | 9   | ir |
| $E_g$    | 10  | 0   | 1    | 1    | 8   | R  |
| $E_u$    | 12  | 1   | 2    | 0    | 9   | ir |

<sup>a</sup> See Table I for the meanings of  $N$ ,  $T$ ,  $T'$ ,  $R'$ ,  $n$ , R, and ir.

In the spectrum of  $Na_3[Co(NO_2)_6]$ , each band shifts by 2–5  $cm^{-1}$  to the higher frequency side with a lowering of temperature. Among them we see a remarkable frequency shift and an intensity enhancement for the band at 214  $cm^{-1}$ . The reason for this feature is not certain. According to the calculation shown in Table IV, this band is assigned to the lattice vibration where the  $Na^+$  ion displaces primarily.

(3)  $K_2Ca[Ni(NO_2)_6]$ ,  $K_2Ba[Ni(NO_2)_6]$ , and  $Na_2Ba[Ni(NO_2)_6]$ .—For these complex salts we have two kinds of outer ions  $M'^+$  and  $M''^{2+}$ . However, the crystal structure of  $K_2Ca[Ni(NO_2)_6]$  and  $K_2Ba[Ni(NO_2)_6]$  is cubic ( $a = 10.34$  and  $10.67 \text{ \AA}$ , respectively), with the space group  $T_h^{3,9}$  as in the case of  $M_3[Co(NO_2)_6]$  ( $M = K, Rb, \text{ and } Cs$ ). No structural analysis has been made for  $Na_2Ba[Ni(NO_2)_6]$ .

TABLE IV  
Calculated and Observed Frequencies  
( $cm^{-1}$ ) of  $Na_3[Co(NO_2)_6]$

| $A_u$      | Calcd | Vib modes                             | $E_u$       | Calcd | Vib modes                             | Obsd     |
|------------|-------|---------------------------------------|-------------|-------|---------------------------------------|----------|
| $\nu_1$    | 1389  | $NO_2$ antisym str                    | $\nu_1'$    | 1391  | $NO_2$ antisym str                    | 1425     |
| $\nu_2$    | 1324  | $NO_2$ sym str                        | $\nu_2'$    | 1324  | $NO_2$ sym str                        | 1333     |
| $\nu_3$    | 802   | $NO_2$ scissor                        | $\nu_3'$    | 801   | $NO_2$ scissor                        | 845, 831 |
| $\nu_4$    | 662   | $NO_2$ wag                            | $\nu_4'$    | 630   | $NO_2$ wag                            | 623      |
| $\nu_5$    | 382   | Co-N str                              | $\nu_5'$    | 441   | Co-N str                              | 449, 372 |
| $\nu_6$    | 270   | $NO_2$ rock and skel def              | $\nu_6'$    | 283   | $NO_2$ rock and $Na''$ lattice        | 276, 249 |
| $\nu_7$    | 219   | $Na''$ lattice                        | $\nu_7'$    | 237   | $Na'$ and $Na''$ lattice              | 214      |
| $\nu_8$    | 179   | Skel def and $Na'$ and $Na''$ lattice | $\nu_8'$    | 194   | $Na''$ lattice and $NO_2$ rock        | 195, 183 |
| $\nu_9$    | 163   | Skel def and $Na'$ and $Na''$ lattice | $\nu_9'$    | 158   | Skel def and $Na'$ and $Na''$ lattice | 147      |
| $\nu_{10}$ | 109   | $Na'$ lattice and skel def            | $\nu_{10}'$ | 133   | Skel def                              | 123      |
| $\nu_{11}$ | 94    | $NO_2$ twist                          | $\nu_{11}'$ | 94    | $NO_2$ twist                          | ...      |

Interionic Potential Constants and Interatomic Distances  
( $Na^+ \cdots O$ )

| Constant | Value, mdyn/ $\text{\AA}$ | Distance | Value, $\text{\AA}$ |
|----------|---------------------------|----------|---------------------|
| $f_1$    | 0.15                      | $q_1$    | 2.55                |
| $f_1'$   | 0.05                      | $q_1'$   | 3.42                |
| $f_2$    | 0.15                      | $q_2$    | 2.62                |

The result of the factor group analysis given in Table I can be applied to the case of  $K_2Ca[Ni(NO_2)_6]$  and  $K_2Ba[Ni(NO_2)_6]$ . The spectra shown in Figure 2 in the region below 500  $cm^{-1}$  reveal seven bands for these complex salts and we have three bands ( $NO_2$  stretching and scissoring vibrations) in the higher frequency region. Therefore, the infrared spectra of these complex salts are consistent with the cubic structure  $T_h^3$ . The calculated frequencies of  $K_2Ca[Ni(NO_2)_6]$  and  $K_2Ba[Ni(NO_2)_6]$  are given in Table V, together with the in-

TABLE V  
Observed and Calculated Frequencies ( $cm^{-1}$ ) of  
 $K_2Ca[Ni(NO_2)_6]$  and  $K_2Ba[Ni(NO_2)_6]$

| $T_h^3$    | $K_2Ca[Ni(NO_2)_6]$ |       |                                  | $K_2Ba[Ni(NO_2)_6]$ |       |                                  |
|------------|---------------------|-------|----------------------------------|---------------------|-------|----------------------------------|
| $F_u$      | Obsd                | Calcd | Vib modes                        | Obsd                | Calcd | Vib modes                        |
| $\nu_1$    | 1355                | 1388  | $NO_2$ antisym str               | 1343                | 1387  | $NO_2$ antisym str               |
| $\nu_2$    | 1325                | 1325  | $NO_2$ sym str                   | 1306                | 1325  | $NO_2$ sym str                   |
| $\nu_3$    | 834                 | 838   | $NO_2$ scissor                   | 838                 | 837   | $NO_2$ scissor                   |
|            |                     |       |                                  | (813)               |       |                                  |
| $\nu_4$    | 458                 | 461   | $NO_2$ wag                       | 433                 | 460   | $NO_2$ wag                       |
| $\nu_5$    | 284                 | 306   | Ni-N str and $NO_2$ rock and wag | 201                 | 304   | Ni-N str and $NO_2$ rock and wag |
| $\nu_6$    | 255                 | 244   | $NO_2$ rock and Ca lattice       | 255                 | 230   | $NO_2$ rock and skel def         |
| $\nu_7$    | 192                 | 196   | K lattice and skel def           | 173                 | 180   | K lattice and skel def           |
| $\nu_8$    | 176                 | 154   | Ca lattice and skel def          | 130                 | 132   | Skel def and K lattice           |
| $\nu_9$    | 135                 | 140   | Skel def and $NO_2$ rock         | (130)               | 107   | Skel def and $NO_2$ rock         |
| $\nu_{10}$ | 105                 | 94    | Ca and K lattice and skel def    | 80                  | 73    | Ba lattice                       |

Interionic Potential Constants and Interatomic Distances

|                            | $K_2Ca[Ni(NO_2)_6]$ |                    | $K_2Ba[Ni(NO_2)_6]$ |                    |
|----------------------------|---------------------|--------------------|---------------------|--------------------|
|                            | $K^+ \cdots O$      | $Ca^{2+} \cdots O$ | $K^+ \cdots O$      | $Ba^{2+} \cdots O$ |
| $f_1$ , mdyn/ $\text{\AA}$ | 0.12                |                    | 0.10                |                    |
| $q_1$ , $\text{\AA}$       | 3.01                |                    | 3.13                |                    |
| $f_2$ , mdyn/ $\text{\AA}$ |                     | 0.15               |                     | 0.12               |
| $q_2$ , $\text{\AA}$       |                     | 2.77               |                     | 2.93               |

terionic potential constants. For  $K_2Ca[Ni(NO_2)_6]$  the vibrations below 200  $cm^{-1}$  show very complicated modes in which lattice modes of  $K^+$  and  $Ca^{2+}$  ions and intramolecular deformation modes are mixed in a com-

plex manner. This may be due to the fact that the intrinsic intramolecular vibration frequencies of  $\text{Ni}(\text{NO}_2)_6^{4-}$  are lower than those of  $\text{Co}(\text{NO}_2)_6^{3-}$ .

In the spectrum of  $\text{Na}_2\text{Ba}[\text{Ni}(\text{NO}_2)_6]$  shown in Figure 2, the band around  $200\text{ cm}^{-1}$  shifts considerably with a lowering of temperature. Such a frequency shift was also seen for the band at  $214\text{ cm}^{-1}$  of  $\text{Na}_3[\text{Co}(\text{NO}_2)_6]$ . Therefore, the band around  $200\text{ cm}^{-1}$  of  $\text{Na}_2\text{Ba}[\text{Ni}(\text{NO}_2)_6]$  may be assigned to the lattice mode related to the  $\text{Na}^+$  ion. The lowest band around  $80\text{ cm}^{-1}$  which also exists in the spectrum of  $\text{K}_2\text{Ba}[\text{Ni}(\text{NO}_2)_6]$  is assigned to the lattice mode related to the  $\text{Ba}^{2+}$  ion.

### Conclusion

The far-infrared bands due to the lattice vibrations and the intramolecular vibrations of the hexanitro complex salts were both interpreted by the normal-coordinate analysis of the crystal as a whole, only the interaction between the outer cations and the oxygen atoms being taken into consideration. Low-temperature spectra yield useful information on the interpretation of the observed bands.

Lattice vibrations due to the displacements of the outer cations relative to the complex ion are observed below  $200\text{ cm}^{-1}$ . Those frequencies change depending upon the mass of the cations and the interionic force constants. In order to establish the characteristic frequencies of the lattice vibrations arising from the outer cations, further investigations on the far-infrared spectra of various types of complex salts are in progress.

### Appendix

For the intramolecular potential,  $V_{\text{intra}}$ , the modified Urey-Bradley force field (MUBFF) has been used

and the use of this type of potential in the vibrational analysis of the complex ions has been fully discussed in several previous papers.<sup>4b,12-14</sup> Force constants used in the present study are summarized in Table VI, where

TABLE VI  
INTRAMOLECULAR POTENTIAL CONSTANTS (MDYN/Å)  
FOR  $\text{Co}(\text{NO}_2)_6^{3-}$  AND  $\text{Ni}(\text{NO}_2)_6^{4-}$ <sup>a</sup>

|  | $\text{Co}(\text{NO}_2)_6^{3-}$ | $\text{Ni}(\text{NO}_2)_6^{4-}$ |
|--|---------------------------------|---------------------------------|
| $F_{\text{dia}}(\text{MN str})$            | 1.50                            | 0.80                            |
| $F_{\text{dia}}(\text{NO str})$            | 9.30                            | 9.30                            |
| $F_{\text{dia}}(\text{NMN def})$           | 1.10                            | 0.60                            |
| $F_{\text{dia}}(\text{ONO def})$           | 1.78                            | 2.00                            |
| $F_{\text{dia}}(\text{MNO def})$           | 0.50                            | 0.40                            |
|  | 0.30 (Na salt)                  |                                 |
| $F_{\text{dia}}(\text{NO}_2\text{ wag})$   | 0.55                            | 0.32                            |
| $F_{\text{dia}}(\text{NO}_2\text{ twist})$ | 0.03 (assumed)                  | 0.03                            |
| $F(\text{N}\cdots\text{N})$                | 0.05                            | 0.20 <sup>b</sup>               |
| $F(\text{O}\cdots\text{O})$                | 3.00                            | 3.00                            |
| $F(\text{M}\cdots\text{O})$                | 0.20                            | 0.10                            |
| $p(\text{NO},\text{NO})$                   | 0.50                            | 0.50                            |

<sup>a</sup> In the Urey-Bradley approach, diagonal elements of the  $\mathbf{F}$  matrix corresponding to the bond stretching modes include  $F$  as well as  $K$  and those for angle deformation modes include  $F$  as well as  $H$ . The off-diagonal elements are expressed in terms of  $F$ .

<sup>b</sup> Taking into account the appreciable interaction between the Ni-N stretching and NMN deformation modes, the effective value of  $F(\text{N}\cdots\text{N})$  was assumed to be large.<sup>4b,12</sup>

$K$ ,  $H$ , and  $F$  denote the bond stretching, the angle deformation, and the repulsion between nonbonded atoms, respectively.  $F_{\text{dia}}$  means the diagonal element of the  $\mathbf{F}$  matrix (potential energy matrix) for the corresponding mode.  $p(\text{NO},\text{NO})$  is the resonance interaction constant. The value of  $p(\text{MN},\text{MN})$  cannot be determined unless the frequencies of the  $g$  species are available.

CONTRIBUTION FROM BELL TELEPHONE LABORATORIES, INC.  
MURRAY HILL, NEW JERSEY 07971

## Rare Earth Orthogallates

BY M. MAREZIO, J. P. REMEIKKA, AND P. D. DERNIER

Received November 9, 1967

Single crystals of the rare earth orthogallates,  $\text{REGaO}_3$  with  $\text{RE} = \text{Sm-Lu}$ , have been synthesized by the decomposition of the respective garnets at high pressure in the presence of a flux. Previously reported crystals of  $\text{LaGaO}_3$ ,  $\text{PrGaO}_3$ , and  $\text{NdGaO}_3$  have been prepared by the flux method at atmospheric pressure. The rare earth orthogallates are isostructural with the rare earth orthoferrites; namely, they have the orthorhombic perovskite-like structure. Their lattice parameters have been calculated by the least-squares method. The parameters  $a$  and  $c$  increase smoothly in going from Lu to La. However, the lattice parameter  $b$  goes through a maximum. It seems that this anomalous variation of the  $b$  parameter can be explained in terms of a variation of the coordination number of the rare earth cation.

### Introduction

In a recent note<sup>1</sup> we reported the synthesis and the crystal structure of  $\text{GdGaO}_3$ ,  $\text{YbGaO}_3$ , and  $\text{YGaO}_3$ . They were synthesized by decomposition at high pressure and high temperature of the respective garnets.

The new orthogallates are isostructural with the respective orthoferrites; namely, they have the orthorhombic perovskite-like structure. An interesting feature is that the rare earth orthoferrites can be synthesized at atmospheric pressure, whereas a pressure greater than 45 kbars is needed to synthesize  $\text{GdGaO}_3$ ,  $\text{YbGaO}_3$ , and  $\text{YGaO}_3$ . This was explained in terms of

(1) M. Marezio, J. P. Remeika, and P. D. Dernier, *Mater. Res. Bull.*, **1**, 247 (1966).